COHERENT DIPOLE SYNCHRO-BETATRON BEAM-BEAM MODES IN ASYMMETRIC RING COLLIDERS

E.A. Perevedentsev and A.A. Valishev,
Budker Institute of Nuclear Physics, 630090, Novosibirsk, Russia

Abstract

Following the work by Hirata and Keil [1] we study the coherent dipole beam-beam effects in asymmetric two-ring colliders and take into consideration the synchrobetatron beam-beam modes arising from the finite bunch length. Their effect on the density of resonances in the tune diagram is shown for the case of different ring circumferences, resulting in reduction of the available tune space.

1 INTRODUCTION

Both analytical and numerical calculations revealed the existence of synchrobetatron modes in the spectrum of coherent dipole betatron oscillations of colliding bunches. These modes have been experimentally detected at the VEPP-2M collider in Novosibirsk [2, 3]. The measured dependence of the mode spectra on the beam-beam parameter ξ is in perfect agreement with the calculations. To simplify calculations, the previous theoretical study was limited to a fully symmetrical case of two bunches with equal parameters (betatron and synchrotron tunes, bunch lengths and intensities). This corresponds to the experimental conditions at VEPP-2M: one electron and one positron bunch circulating in a common magnetic system.

Recently, a number of circular collider projects have been proposed with significant asymmetry between the rings. In the GSI project of electron-ion collider [4] the ratio of the electron and ion ring circumferences ranges from 1:6 to 1:10 at different ion beam energies. The betatron and synchrotron tunes also differ noticeably.

A simplified treatment of coherent beam-beam motion is available for dipole beam-beam modes, provided that the beam-beam force is linearized, [1] and references therein. For colliders with different circumference lengths (in fact, the revolution frequency of one of the rings is a multiple of another) the resonant instabilities seem to be the most important. For strong enough beam-beam parameters, multiple stopbands of linear coupling resonances of the coherent dipole beam-beam modes occupy a significant portion of the tune space together with the integer and half-integer coherent beam-beam stopbands, thus leaving not too much space for stable operation.

In the present paper, following [1] we first perform an eigenvalue analysis of the coherent dipole beam-beam modes of the zero-length bunches, for the case of 6-fold multiplicity of the revolution frequency of the electron ring with respect to that of the ion ring, to find the stable regions in the ν_e–ν_i tune space (Section 2). An enhanced model of the coherent synchrobetatron beam-beam modes for the case of different bunch parameters in two equal circumference rings is discussed in Section 3. Section 4 gives the results of the complete model consideration, taking account of the synchrobetatron modes in a system with multiple beam revolution frequencies.

2 RIGID BUNCH CALCULATION

Since we use the linearized beam-beam approximation, it is convenient to use the matrix eigenvalue analysis to study the system stability. In this section we shall consider the bunches to be thin rigid discs, each described by the normalized betatron coordinate and the respective momentum. The system of one electron and six ion bunches is characterized with the 14-vector of coordinates and momenta where the first two elements correspond to the electrons while the rest present the ion bunches in their sequence along the ring azimuth. The 14×14 matrix representing transformation of the vector over one turn in the electron ring is

$$M_\beta = \begin{pmatrix} M_e & 0 & \dots & 0 \\ 0 & M_{i/6} & & \vdots \\ \vdots & & \ddots & 0 \\ 0 & \dots & 0 & M_{i/6} \end{pmatrix},$$

where M_e and $M_{i/6}$ are the usual 2×2 betatron matrices with the betatron phase advances $2\pi\nu_e$ and $2\pi\nu_i/6$ respectively. Indices e and i label betatron tunes of the electron and ion rings.

The beam-beam interaction between the electron bunch and ion bunch No. 1 is expressed using the kick matrix

$$M_{e,1} = \begin{pmatrix} 1 & 0 & 0 & 0 & \dots & 0 \\ -2\pi\xi_i & 1 & 2\pi\xi_i & 0 & & \vdots \\ 0 & 0 & 1 & 0 & & \\ 2\pi\xi_e & 0 & -2\pi\xi_e & 1 & & \\ 0 & & & & & \vdots \\ \vdots & & & & \ddots & 0 \\ 0 & \dots & & \dots & 0 & 1 \end{pmatrix},$$

here ξ_e and ξ_i are the beam-beam parameters of the electron and ion beams. The coherent beam-beam kick is $2\pi\xi$ since the beams have Gaussian distribution in the transverse direction.

After the second turn the electron bunch collides with ion bunch No. 2. This interaction is represented by matrix

$M_{e,2}$. Next follows another turn and so on. The complete period is given with the matrix M_{ei} which is the product of 6 betatron transformations M_β with consecutive collisions.

$$M_{ei} = M_{e,6} \cdot M_\beta \ldots M_{e,1} \cdot M_\beta \ .$$

With the beam-beam parameters of intentionally exaggerated value, $\xi_i = 0.1$, $\overline{\xi}_e = 0.03$, and variation of the ion bunch population of 20 percent, we plot the sum of absolute values of the coherent dipole beam-beam mode increments as a function of the tunes in Fig. 1. The large values

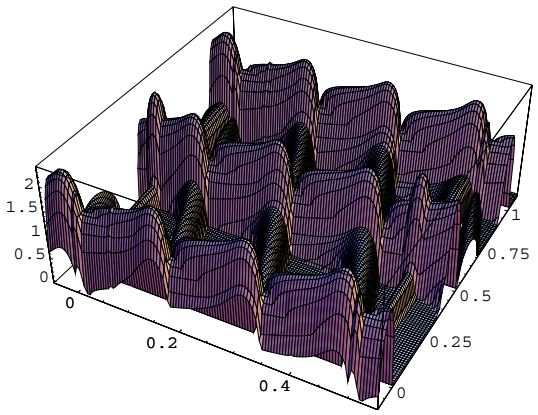

Figure 1: Sum of the dipole beam-beam modes increments as a function of the tunes: abscissa is the electron ring tune ν_e (mod 1/2), ordinate is the ion ring tune ν_i (mod 1).

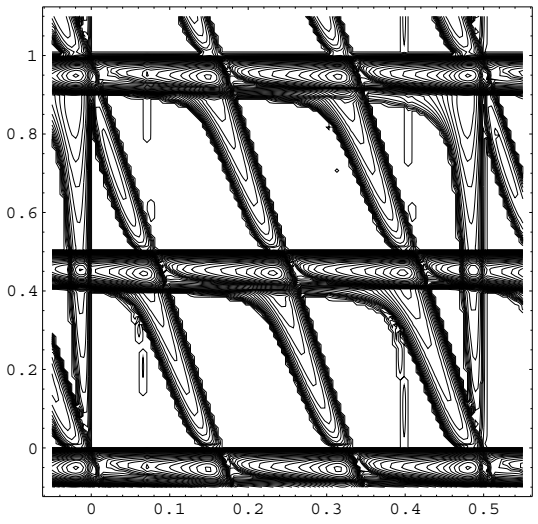

Figure 2: Same as in the previous figure, in the form of the contour plot, showing the stable regions in between the resonance stopbands.

of the increments in the half-integer, integer and coupling stopbands imply that these resonance should be carefully avoided in operation. The small increments of the 1/12, 5/12 and other $n/12$ resonances, which are due to unequal population in the ion bunches leave some hope that these can be stabilized for instance by the Landau damping resulting from the beam-beam tune-spreads and the Laslett tune-spread, even if the working point hits these lines.

Fig. 2 shows the contour plot of the stopbands resulting from the linear coherent dipole beam-beam resonances in the same conditions as in Fig. 1. One can draw a preliminary conclusion that the multiplicity 6 (and even somewhat higher) is not preclusive for the stable beam-beam operation.

3 SYNCHROBETATRON MODES

Now we come back to equal revolution frequencies. For a finite-length bunch collisions the frequency spectrum analysis of the coherent beam-beam modes with the account of the bunch deformation over the interaction length is done using the circulant matrix formalism [5]. Assuming the disruption parameter $4\pi\xi\sigma_s/\beta^*$ value (or, in other words, the beam-beam "wake" variation over the bunch length σ_s) to be small, we apply the hollow beam model, when all particles in the bunch have equal synchrotron oscillation amplitudes and are evenly spread over the synchrotron phase. Following [3] the bunch is divided into N mesh elements, each characterized by its transverse dipole moment and its synchrotron phase. The dipole moment of the ith mesh, $i = 1 \ldots N$, is proportional to the transverse displacement x_i of the centroid of the particles populating this mesh, times the portion N_b/N of the bunch intensity, N_b, per mesh. The betatron motion will be described in terms of the normalized betatron variables, x_i and p_i, where p_i is the respective momentum. Thus $2N$ variables will be needed to characterize synchrobetatron motion in each bunch. They form a $2N$-vector, where x_i and p_i are listed in the order corresponding to the mesh number, according to its synchrotron phase.

The synchrobetatron oscillations of N elements forming a bunch are represented by the $2N \times 2N$ matrix M, which maps the above vector over the collider arc,

$$M_{sb} = C \otimes B \ ,$$

where $\otimes$ denotes the outer product, B is the usual 2×2 betatron oscillation matrix, and C is the $N \times N$ circulant matrix. Since it represents the synchrotron oscillations, its elements depend on the synchrotron tune ν_s.

The basic advantage of the circulant matrix is that it transforms dipole moments inside the mesh elements and leaves their longitudinal positions unchanged. This facilitates coding of the interaction between the particles.

Free synchrobetatron oscillations of the system of two noninteracting bunches is described by the $4N \times 4N$ matrix

$$M_2 = \begin{pmatrix} M_{sb1} & 0 \\ 0 & M_{sb2} \end{pmatrix} \ .$$

The betatron and synchrotron oscillation parameters in matrices M_{sb1} and M_{sb2} are arbitrary.

The beam-beam interaction is expressed via the system of thin lens and drift matrices which represent relative longitudinal positions of the elements. Collision of the particles No. i in one bunch and No. j in the other changes their momenta according to the formula

$$\Delta p_i = -2\pi\xi_2(x_i - x_j) \,,$$
$$\Delta p_j = -2\pi\xi_1(x_j - x_i) \,,$$

where ξ_1 and ξ_2 are the beam-beam parameters of the two bunches. Multiplication of the consecutive kick matrices followed by free drifts gives the complete $4N \times 4N$ beam-beam matrix.

It was shown that no transverse mode coupling occurs in the beam-beam system with fully symmetrical bunches [5, 2]. Here we present the results of coherent synchrobetatron beam-beam mode spectra calculation within the framework of the above described asymmetrical model for $N = 5$. Figure 3 shows the dependence of the mode tunes on ξ for the case of equal betatron tunes and bunch intensities, while the synchrotron tunes differ.

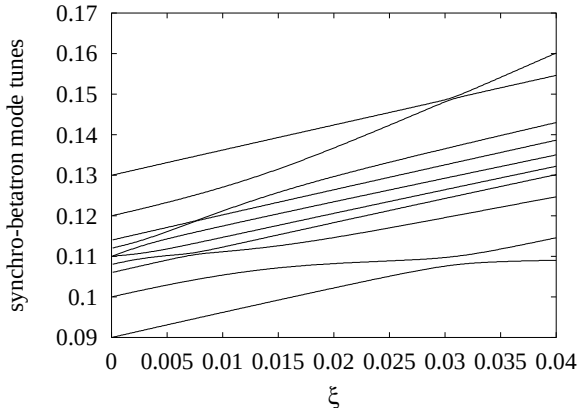

Figure 3: Synchrobetatron mode tunes vs. ξ. $\nu_{\beta,1} = 0.11$, $\nu_{\beta,2} = 0.11$, $\nu_{s,1} = 0.01$, $\nu_{s,2} = 0.002$, $\sigma_1 = \sigma_2 = \beta^*$.

In Figs. 4 and 5 the spectra with equal synchrotron tunes and different betatron tunes are plotted. In Fig. 4 the betatron tune split is small relative to the synchrotron tune, and the lower order modes overlap; in Fig. 5 they are fully decoupled.

Figure 6 gives the mode spectra with equal intensities, synchrotron and betatron tunes, and the bunch length of one bunch two times less then the others.

These calculations do not display any fundamental difference as compared to the symmetrical case. The modes do not intersect, their repulsion is due to coupling of the synchrobetatron modes via the collective beam-beam response. There is no coherent instability in the whole range of ξ when the tune of neither mode reaches 0, 0.5 or a sum resonance.

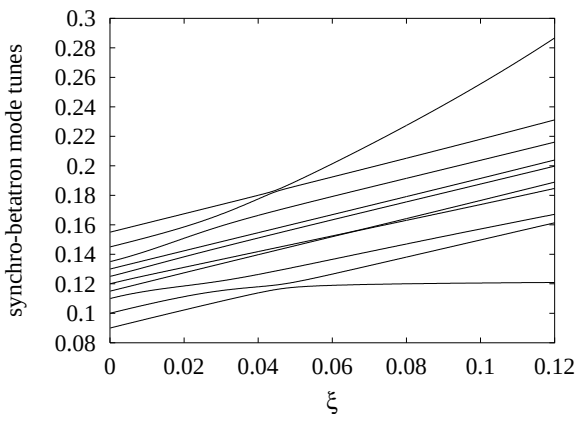

Figure 4: Synchrobetatron mode tunes vs. ξ. $\nu_{\beta,1} = 0.11$, $\nu_{\beta,2} = 0.135$, $\nu_{s,1} = 0.01$, $\nu_{s,2} = 0.01$, $\sigma_1 = \sigma_2 = \beta^*$.

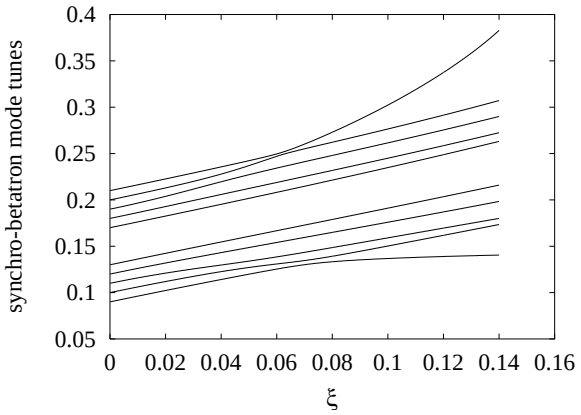

Figure 5: Synchrobetatron mode tunes vs. ξ. $\nu_{\beta,1} = 0.11$, $\nu_{\beta,2} = 0.19$, $\nu_{s,1} = 0.01$, $\nu_{s,2} = 0.01$, $\sigma_1 = \sigma_2 = \beta^*$.

4 COMPLETE MODEL

To describe the beam-beam interaction of the beams with different parameters and revolution frequencies we use the model which is the combination of the approaches presented in Sections 2,3. For the ring circumference ratio 1:6 and maximum considered synchrotron wavenumber of ± 2, the system state is characterized by the 70-vector of the mesh coordinates and momenta. The first 10 elements of this vector describe the 5 particles of the electron bunch, then follow 5 particles of the first ion bunch and so further. The synchrobetatron transformation of the vector over one revolution in the electron ring is done with the matrix similar to M_β where instead of the 2×2 betatron matrices the 10×10 synchrobetatron ones are substituted.

The beam-beam interaction is coded as described in Sections 2,3, taking into consideration the correct interaction sequence and the longitudinal positions of the particles with respect to the bunch center.

In Figs. 7,8 the mode tunes and increments are plotted vs. the beam-beam parameter ξ with realistic parameters of the electron and ion bunches. The betatron tune in the

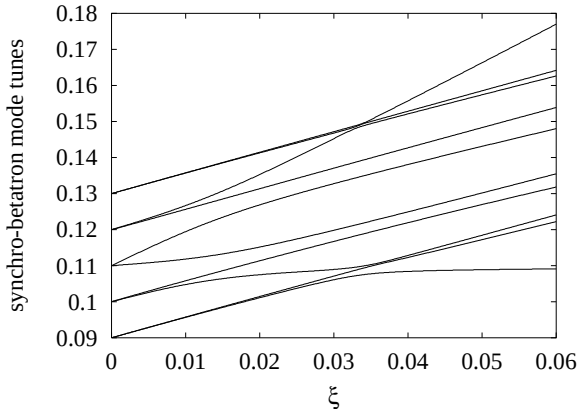

Figure 6: Synchrobetatron mode tunes vs. ξ. $\nu_{\beta,1} = 0.11$, $\nu_{\beta,2} = 0.11$, $\nu_{s,1} = 0.01$, $\nu_{s,2} = 0.01$, $\sigma_{s1} = 2\sigma_{s2} = \beta^*$.

electron ring is 0.1, which gives the phase advance over 6 revolutions of $2\pi \cdot 0.6$. Hence, the 0-mode corresponding to electrons shows in the spectrum as the aliased mode at $0.5 - (0.6 - 0.5) = 0.4$. When this mode couples with the ion 0-mode the instability occurs due to synchrobetatron sum resonance.

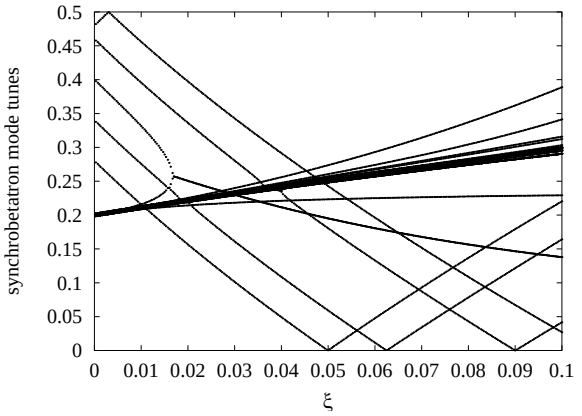

Figure 7: Synchrobetatron mode tunes vs. ξ in asymmetric collider. Circumference ration 1:6, $\nu_{\beta,e} = 0.1$, $\nu_{\beta,i} = 0.2$, $\nu_{s,e} = 0.01$, $\nu_{s,i} = 0.001$, $\sigma_s = 0.7\ \beta^*$.

In Figure 9 the stability diagram is plotted in the ν_e, ν_i coordinates for fixed ξ value and with synchrotron tunes of the electron and ion beams equal to those in Figs. 7,8. No significant reduction of the stable tune space is seen due to the synchrobetatron resonances.

The same calculation with the intentionally large synchrotron tunes of 0.05 shows a large number of synchrotron sideband resonances in the stability diagram (Fig. 10).

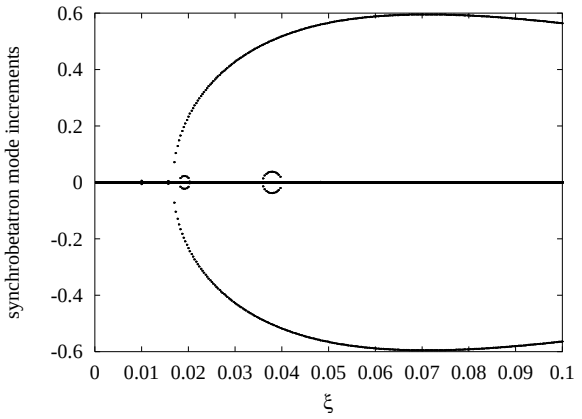

Figure 8: Synchrobetatron mode increments per turn vs. ξ in asymmetric collider. Parameters are the same as in Fig. 7.

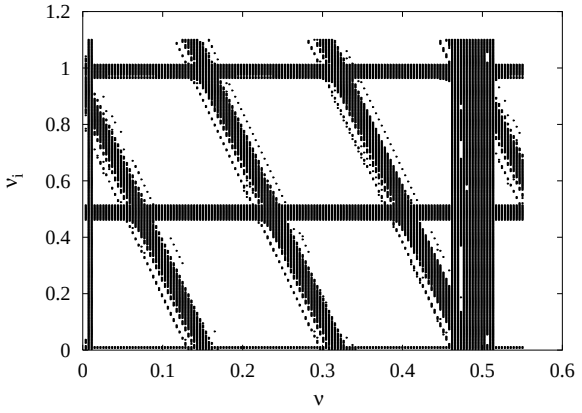

Figure 9: Stability tune diagram. $\xi = 0.01$, $\nu_{s,e} = 0.01$, $\nu_{s,i} = 0.001$, $\sigma_s = \beta^*$.

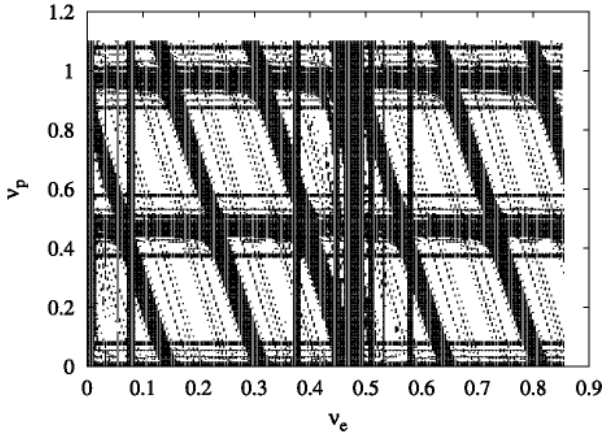

Figure 10: Stability tune diagram. $\xi = 0.02$, $\nu_{s,e} = 0.05$, $\nu_{s,i} = 0.05$, $\sigma_s = 0.7\ \beta^*$.

5 CONCLUSION

In circular colliders with unequal (but multiple) revolution periods the dipole beam-beam resonances form a grid in the tune space and can cause a problem in optimizing the collision working point. If the multiplicity is too high (≥ 10), the beam-beam footprint will be limited by the lines of these resonances unless the dipole beam-beam modes are damped by a transverse feedback. The latter can not completely cure the synchrobetatron sidebands of these resonances arising from the finite length of the colliding bunches, however in current projects for electron-ion colliders the sidebands do not cause a strong reduction of the tune space.

6 REFERENCES

[1] E. Keil, CERN LEP note 226, (1980);
K. Hirata, E. Keil, *Nucl. Instr. Meth.* **A 292**, 156 (1990);
K. Hirata and E. Keil, *Particle Accelerators* **56**, 13, (1996).

[2] E.A. Perevedentsev and A.A. Valishev, *Phys. Rev. ST-AB* **4**, 024403 (2001);
E.A. Perevedentsev and A.A. Valishev, in Proc. 2000 European Particle Acc. Conf., Vienna (2000), p. 1223;
E.A. Perevedentsev and A.A. Valishev, in Proc. 2000 Int. Computational Acc. Phys. Conf., Darmstadt (2000).

[3] I.N. Nesterenko, E.A. Perevedentsev, A.A. Valishev, these proceedings.

[4] I.A. Koop et al., "Conceptual Design of an Electron-Nucleus Scattering Facility at GSI.", BINP internal report (unpublished).

[5] E.A. Perevedentsev, in Proc. 1999 Particle Accelerator Conf., New York (1999), vol. 3, p.1521;
E.A. Perevedentsev, in Proc. Int. Workshop on Electron-Positron Factories, Sept. 21-24 1999, Tsukuba, KEK Proceedings 99-24, Feb. 2000.